Journal of Marine Science and Application (2022) 21: 192-204
https://doi.org/10.1007/s11804-022-00308-4

RESEARCH ARTICLE

Experimental Study on Tilt Adjustment Technique of Tripod Bucket Jacket Foundation for Offshore Wind Turbine in Sand

Puyang Zhang[1, 2], Yuxuan Ma[1, 2], Conghuan Le[1, 2] and Hongyan Ding[1, 2]

Received: 29-Jun-2022 / Accepted: 15-Sep-2022

Abstract

For the tripod bucket jacket foundations used in offshore wind turbines, the probable critical tilt angles should be avoided during tilt adjustment operation. Thus, these critical values must be identified by engineers, and remedial techniques must be established prior to the occurrence of the problem. Model tests were carried out for typical tilting conditions of tripod bucket foundations, which were allowed to tilt freely at various penetration depths without interruption by manual operation. After the foundation ceased its tilting, some measures, such as water pumping, water injection, air injection, or a combination of the above methods, were enabled for adjustment. The research results showed two critical values in the tilting state of the tripod bucket jacket foundation, namely the terminal and allowable angles. In the installation condition, the terminal angle was negatively correlated with the initial penetration depth, but the opposite was observed with the removal condition. The allowable angle was less than or equal to the terminal angle. The allowable angle in the installation was related to the terminal angle. The critical angles all varied linearly with the initial penetration depth. When tilting during installation, adjustment measures can be used in the order of high drum pumping, low drum water injection, high drum pumping and low drum water injection, air injection, and exhaust. When tilting during removal, the sequential use of low drum water injection, air, and exhaust was applied. For buckets that were sensitive to angle changes, adjustment measures of the "point injection" mode can be selected.

Keywords Tripod bucket jacket foundation; Tilt adjustment; Penetration and removal; Terminal angle; Allowable angle; Offshore wind turbine

1 Introduction

Offshore wind power has received increasing attention from many countries (Ren et al., 2022). A variety of foundation types have been proposed (Zhang et al., 2022); among these foundation types, the suction bucket foundation is one of the most promising (Achmus and Schroeder, 2014). A suction bucket foundation typically consists of a steel cylinder that is closed at the top. Steel cylinders have been used as foundations of jacket structures and can be converted into a composite bucket foundation by the addition of subdivision panels inside the bucket (Zhang et al., 2016). Suction bucket foundations originated from offshore oil and gas exploration platforms and can be divided into suction buckets, suction anchors, and suction piles based on application scenarios and sizes. With the development of renewable energy resources in recent years, the suction bucket foundation has been "transplanted" to the wind energy industry as the bottom support structure for offshore wind turbines because of its features, such as low cost, high bearing capacity, convenient construction, and environmental friendliness. Many scholars (Wang et al., 2019; Wu et al., 2020; Jia et al., 2018; Chen et al., 2021)

Article Highlights

- Model tests were carried out for typical tilting conditions of tripod bucket foundations;
- The terminal and allowable angles are two critical values in the tilting state;
- The water pumping/injection, air injection, or a combination of the above methods are enabled for adjustment.

✉ Puyang Zhang
zpy_td@163.com

[1] State Key Laboratory of Hydraulic Engineering Simulation and Safety, Tianjin University, Tianjin 300072, China

[2] School of Civil Engineering, Tianjin University, Tianjin 300072, China

have conducted research on suction bucket foundations, focusing on different soil layers and foundation types, and mainly included the bearing capacity and formation mechanism of the water layer, seepage characteristics and failure mechanism of soil plug, penetration resistance and critical suction, control of applied suction, and strategy of tilt adjustment. The above problems must be solved to avoid the occurrence of unstable states in the construction process, allowing it to meet the design requirements and maximize the technical advantages and economic benefits of the bucket foundation.

For practical projects, effective installation is the premise of the above exploration; however, the tripod bucket jacket foundation will inevitably be inclined during the penetration process due to various reasons, such as uneven geology and construction operations (Zhang et al., 2013a). Tilt adjustment is the main characteristic of the bucket foundation, with "suction" as the driving force for penetration. Currently, many countries have their own specifications regarding verticality after installation. DNV require that the inclination angle should not exceed ±0.5° (DNV, 2005). Engineers must understand not only the construction objectives but also the critical safety value, which may be observed during the installation of the tripod bucket foundation, and therefore, an emergency solution should be in place if the critical value occurs. This requirement should be emphasized in the disclosure of construction safety technology. Ding et al. (2004) demonstrated the feasibility of implementing a negative-pressure leveling operation when the penetration depth of the tripod bucket jacket foundation is shallow; however, when the penetration depth is deep, a positive pressure must be applied to each bucket separately. Jia (2018), Jia et al. (2018) and Zhang (2018) conducted research on composite and multi-bucket jacket foundations, respectively, including studying leveling strategy and the relationship between penetration depth and tilt adjustment; they concluded that the greater the amount of mud entering, the more difficult the leveling operation is. Zhang et al. (2013b) believed that by using air extraction or water injection, the inclination angle of the tripod bucket jacket foundation can be reduced from 6.28° to 0.5°, and the inclination angle of 6.6° can still be reduced to 1.29° even if the foundation has penetrated a hard clay layer; multiple tilt adjustments may result in high soil plugs in the bucket, affecting the final penetration depth. Therefore, tilt adjustment should be performed immediately during the initial stage of penetration. Referring to the methods and conclusions of the predecessors, a more systematic study on the critical angle and tilt adjustment strategy for the tripod bucket jacket foundation was carried out to serve the engineering practice.

The construction site features complex and changing situations. Improper geological survey and operation may result in the failure of foundation installation, necessitating its removal. Therefore, the tilt adjustment with the removal process must be studied. Zhang et al. (2013c) analyzed the change in the removal resistance of the tripod bucket foundation based on the field prototype test and compared it with the penetration resistance during the initial installation. Little research has been conducted on the removal of tripod bucket jacket foundations, and they focused on the resistance of removal. In summary, this paper aimed to explore the critical angle value of the tripod bucket jacket foundation during the installation and removal process and discuss strategies to adjust these critical angles.

2 Test program

2.1 Test model and soil

As shown in Figure 1, the tripod bucket jacket foundation was selected for the test model, which was composed of three buckets and one model jacket. Geometric, kinematic, and dynamic similarities should be satisfied in the design of the model test. The model scale was 1:50, with steel as the main material, and the top cover of the bucket was made of plexiglass with improved visibility. The height of the prototype bucket was 12.5 m, the diameter was 15 m, the distance between buckets was 30 m, and the skirt wall thickness was 40 mm. Considering the manufacturing accuracy and steel strength, the thickness of the model skirt wall was 1.5 mm. The height of the model jacket was designed to accommodate transfer with a crane.

Table 1 shows the detailed dimensions of the test model.

Based on the "Geotechnical Test Method Standard" (CNS, 2019), a series of laboratory geotechnical tests was carried out, and the resulting data are presented in Table 2. The elastic modulus was determined by a triaxial compression test with a laboratory triaxial instrument.

2.2 Experimental equipment

Figure 2 shows a schematic of the power system for the tripod bucket jacket foundation. For water pumping or air-injection operation, the order of pipeline connection was as follows: intelligent air pump, anti-overflow bucket, ventilation weighing bucket, pipeline control valves, and tripod bucket jacket foundation. The intelligent air pump had two ports: intake and exhaust ports. When pumping water, the anti-overflow bucket port was near the pump connected to the intake port, shown as the solid line near the intelligent air pump. However, when air needed to be injected, the upper port of the anti-overflow bucket was connected to the exhaust port, shown as the dotted line near the intelligent air pump. For water-injection operation, the sequence connection of the pipeline was as follows: water-injection pump, pipeline control valves, and tripod bucket jacket

(a) Schematic of the three-dimensional model

(b) Engineering picture

Figure 1 Schematic of the laboratory model

Table 1 Dimensions of the model unit: mm

Diameter of bucket	Height of bucket	Thickness of bucket	Center distance of bucket	Height of jacket
300	250	1.5	600	430

foundation. Continuous operation of the power system, switching of pipeline connection sequence and valve regulation, and the penetration, removal, and tilt adjustment for the foundation can be realized. Five holes were reserved at the top of each bucket to match the system. Among these holes, four were used to connect pipelines, and the remaining one was used as an exhaust hole/observation hole. One of the four pipeline connection holes was a spare.

Figure 3 shows the arrangement of the superstructure device for the tilt adjustment test. Given the need to monitor the change in the inclination angle of the foundation in real time, the inclinometer was placed at the top of the jacket. In addition, to prevent the center of gravity of the test model from moving up in the tilt adjustment test, we used a thinner screw as the tilt reference indicator. A displacement meter was used to measure the initial penetration/removal depth.

The soil pressure around the skirt was monitored, and thus, the soil pressure sensor was arranged on the outer wall of the skirt, which was 50 mm away from the tip. Given the test purpose, this test did not collect the changes in soil pressure when the bucket penetrated by self-weight. The statistical results of multiple pre-penetrations showed that the average self-weight penetration depth was 50 mm. Operationally, if the soil pressure sensor was placed at a distance of 0 mm from the tip, it would be easily bumped during the model handling process. Therefore, the soil pressure sensor was placed 50 mm away from the tip of the bucket. As shown in Figure 4, the red soil pressure sensor was named as the outer of the outer for the No. 1 bucket (OO1), the orange soil pressure sensor as the inner of the outer for the No. 1 bucket (IO1), and so on. The abbreviations of the yellow, purple, pink, and purple sensors were OO2, IO2, OO3, and IO3, respectively.

As shown in Figure 5, the water pressure sensors were placed inside and outside the bucket top cover. During the tilt adjustment test, the elevations of the three buckets could be inconsistent; as shown in Figure 5, the water pressure sensors were placed inside and outside each bucket top cover. This was because the elevations of the three buckets could be inconsistent during the tilt adjustment test.

2.3 Design of experiment conditions and procedure

In the process of penetration and removal, there may be three types of inclination. The first case is that the elevation of one bucket is higher than that of the other two buckets with the same elevation (OBH), and the second case is that the elevation of one bucket is lower than that of the others with the same elevation(OBL), and the last case is that the elevations of all three buckets are different (TBD). Among them, case 1 and case 2 are two extreme cases, and case 3 is a general case in between. The three

Table 2 Parameters of soil

Type	Relative compaction	Elastic modulus (MPa)	Internal friction angle (°)	Cohesion (kPa)	Maximum dry density (g/cm^3)	Minimum dry density (g/cm^3)	Permeability coefficient (cm/s)
Saturated fine sand	0.58	18	32.5	13.2	1.50	1.28	0.039

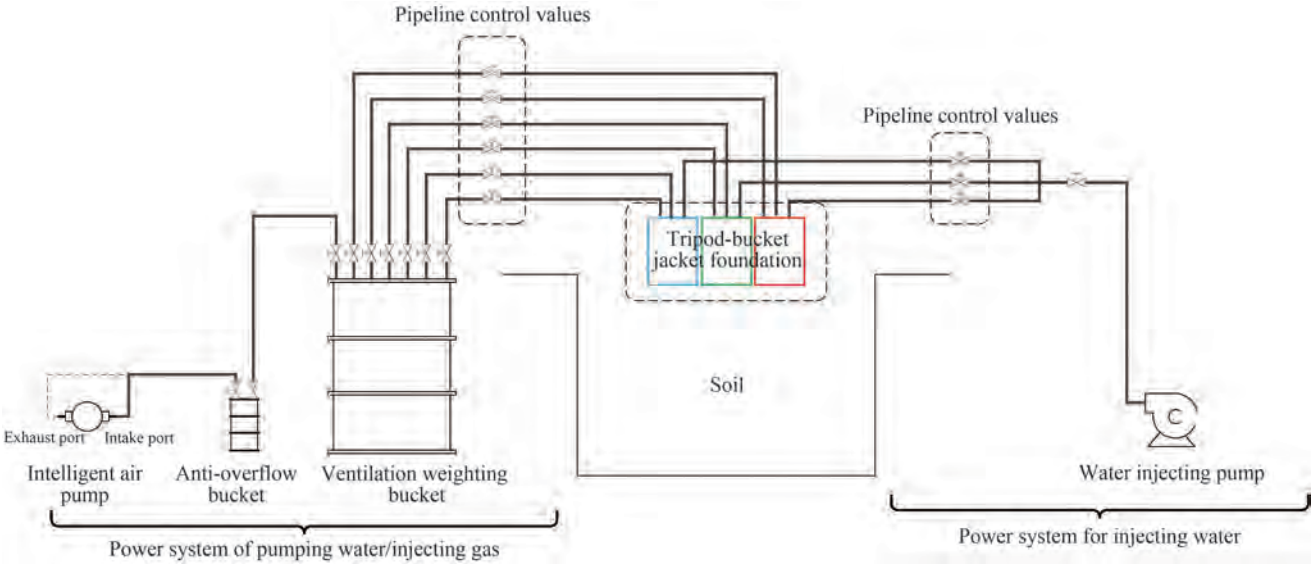

Figure 2 Power system for the tripod bucket jacket foundation

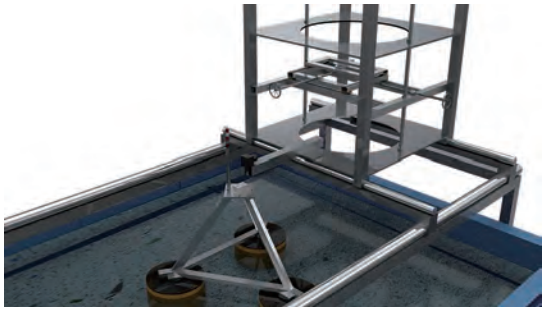

Figure 3 Arrangement of the superstructure device for the tilt adjustment test

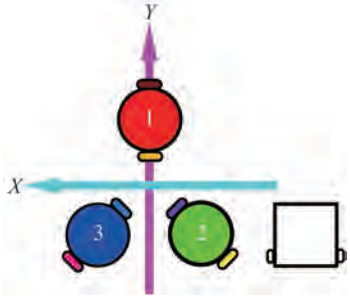

Figure 4 Layout of the soil pressure sensor

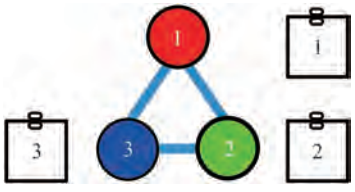

Figure 5 Layout of the water pressure sensor

cases are shown in Figures 6(a), (b) and (c) in turn.

To explore the critical angle and strategy of tilt adjustment for tripod bucket jacket foundation, we performed the specific steps as follows. First, we applied suction (for penetration) or lift (for removal) to the tripod bucket jacket foundation after reaching a certain depth of mud penetration. The detailed process is as follows. The foundation was placed in the soil box by a crane, with the reserved holes at the top of the bucket open. This operation can allow the foundation to penetrate into the soil by self-weight. After the self-weight penetration reached its limit, the foundation was connected to the power system, and the reserved holes were closed. The foundation continued to penetrate to a certain depth by pumping water. Second, in accordance with the design conditions, the inclination was undisturbed until the change in monitoring angle was terminated, after which the application of suction or lift was stopped. Third, after waiting for 10–15 min, tilt adjustment for the foundation was conducted, and whether the foundation can be adjusted within a specified range was observed ("Design regulations on subgrade and foundation for WTGS of wind power" require that the slope rate should not exceed 3‰).

3 Analysis of critical angles

As shown in Figures 7(a) and 7(b), the tripod bucket jacket foundation in the soil was subjected to the soil pressure from the surrounding and core soils. The soil pressure sensors of one bucket were all preset outside the skirt, that is, not only on the same longitudinal section of the bucket but also on the same transverse section. The intersection of two cut planes is called the reference line. For the same bucket, the outer soil pressure minus the inner soil pressure is called the difference in soil pressure (DSP). The

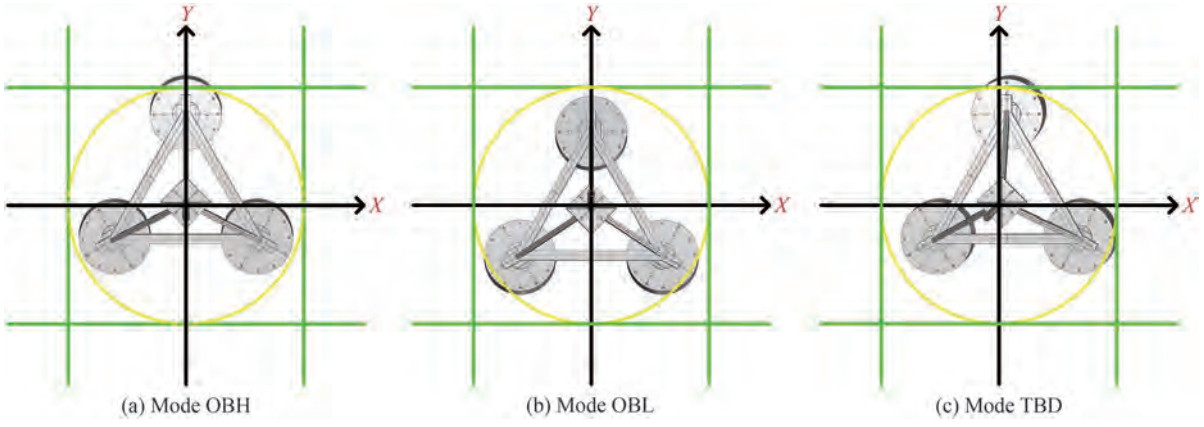

Figure 6 Schematic of tilt mode

time-history change curve of the DSP reflects the change in the soil pressure on the relatively strong side, which is the resultant force on the reference line. From the definition of DSP, the positive direction is the value of outer soil pressure that is greater than the value of inner soil pressure, and vice versa for the negative direction. An inflection point on the time-history curve of DSP represents the weakening or strengthening of the resultant force of a single bucket. Furthermore, the appearance of the inflection point of DSP indicates that the soil around the bucket has been damaged. Thus, the soil cannot continue to meet the increase in bearing capacity.

We obtained the resultant force for the DSP of No. 1, No. 2, and No. 3 buckets. All three DSPs were on the same plane (the inclination angle of the plane is the inclination angle of the tripod bucket jacket foundation measured by the inclinometer). Thus, the resultant force can be decomposed into a rectangular coordinate system (the direction of the specified coordinate system is the same as that of the inclinometer coordinate system) and is called the component of the resultant DSP in the *X* direction (CRDSP-*X*) and the component of the resultant of DSP in the *Y* direction (CRDSP-*Y*) (Figure 7(c)). From the previous discussion, when one of the time-history curves of CRDSP-*X* or CRDSP-*Y* reaches the inflection point, the surrounding soil of the entire foundation is destroyed. The angle corresponding to this inflection point is defined as the allowable angle for the tripod bucket jacket foundation. In addition, the angle at which the foundation ends inclination is the terminal angle.

3.1 Critical angles of penetration

Figure 8 shows the time-history curve of CRDSP. For the terminal angle, the values of modes OBH and OBL were greater than those of mode TBD at the same depth. Therefore, we considered the values of modes OBH and OBL in this research. Further, the curve of modes OBH and OBL considered the angle in the *Y* direction.

For the penetration at different depths (50, 100, and 150 mm in sequence), the terminal angles of the mode OBH were 11.475°, 6.719°, and 4.422°, and the allowable angles were 7.764°, 4.1°, and 0.857°, respectively. At different depths, the ratios of the terminal angle to the allowable an-

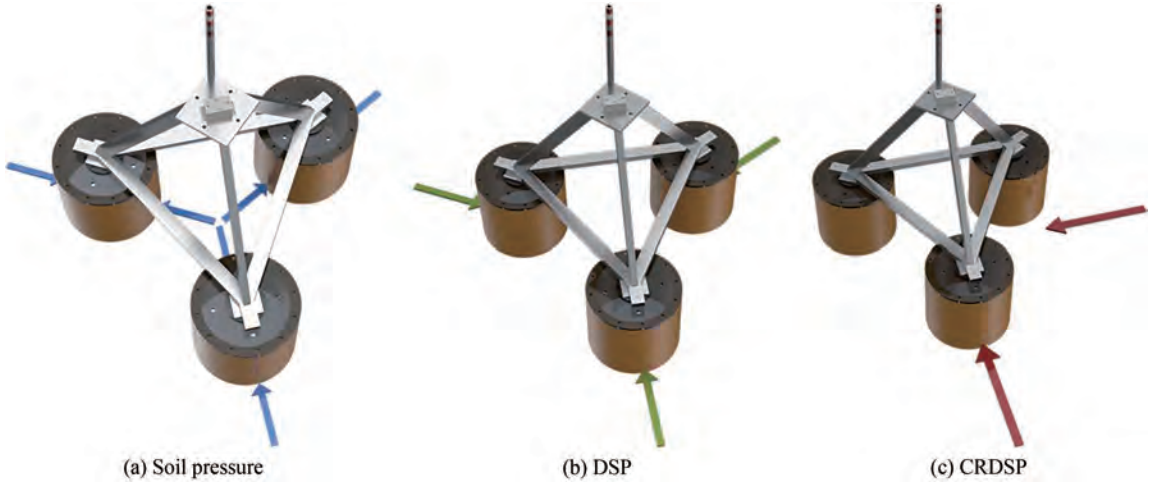

Figure 7 Treatment for soil pressure (arrows represent force)

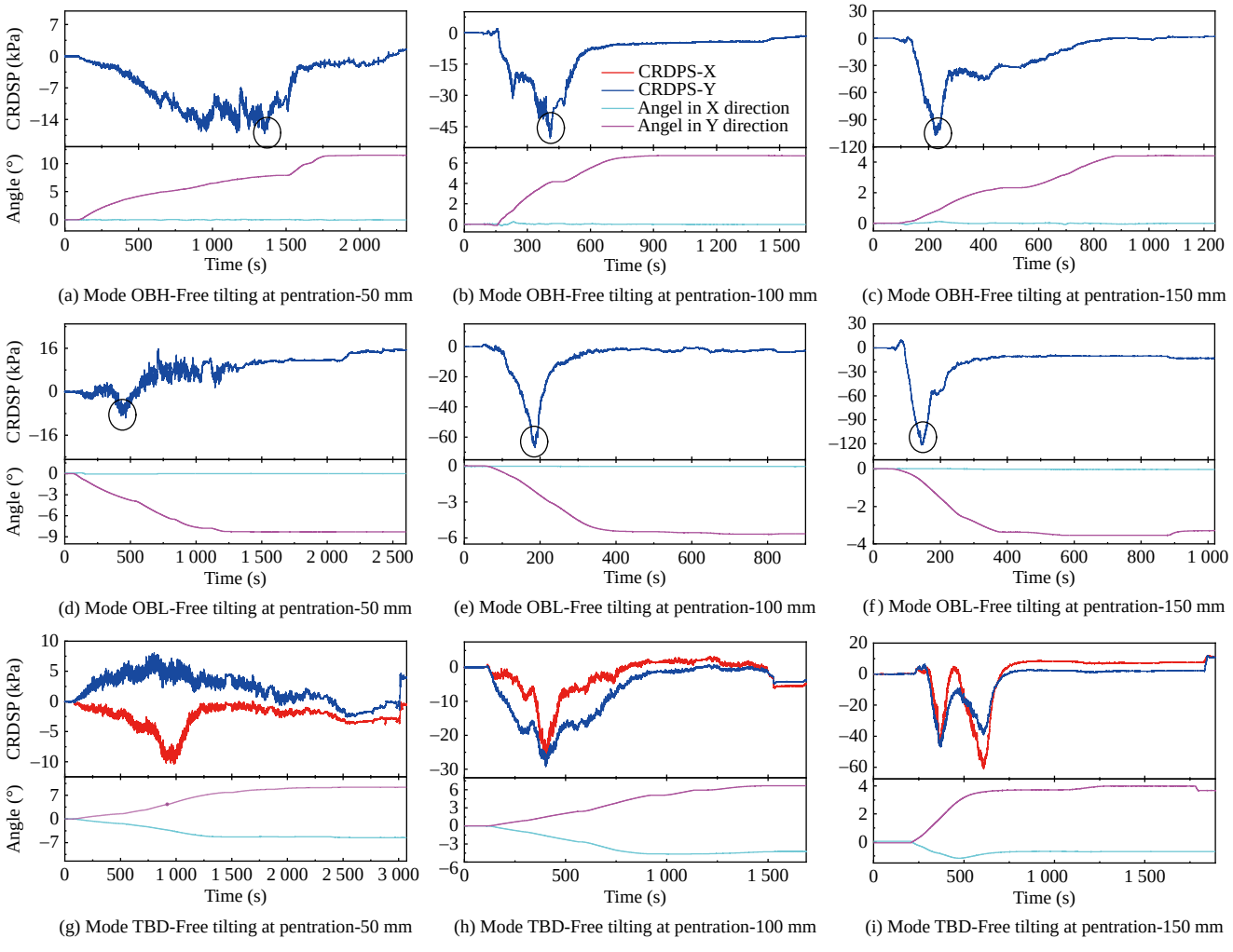

Figure 8 Free tilting time-history curves of CRDSP and angle during penetration at different depths

gle were 1.48, 1.64, and 5.16. In the case of penetration, for the mode OBL at different depths, the terminal angles were −8.305°, −5.524°, and −3.54°, and the allowable angles were −3.46°, −2.12°, and −0.649°, respectively. The ratios of the terminal angle to the allowable angle were 2.3, 2.61, and 5.45. Figure 9 plots the above data about critical angles into an envelope diagram.

We performed linear fitting on the curve in Figure 9 to obtain the analytical formula of the critical angle envelopes (Table 3).

3.2 Critical angles of removal

Figure 10 shows the time-history curve for removal. The figure describes CRDSP. As shown in Figures 10a, 10b, and 10c, with the increase in depth, the drop point of CRDSP for the mode OBH showed a tendency to approach the origin. Thus, with the increase in depth, the difference between the allowable and terminal angles increased. In particular, at a depth of 50 mm, the angle and CRDSP curves declined almost simultaneously. Thus, the

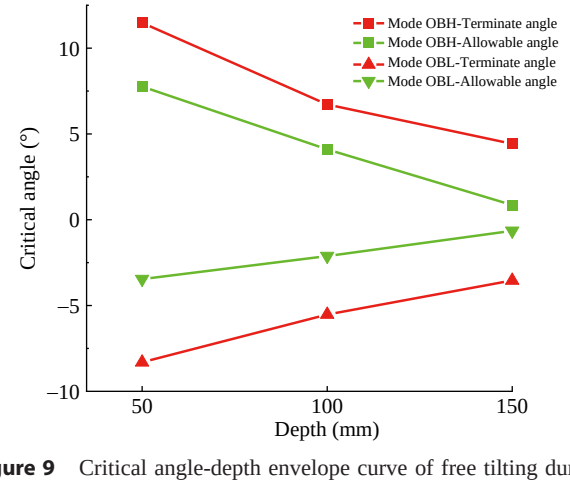

Figure 9 Critical angle-depth envelope curve of free tilting during penetration

terminal and allowable angles were the same at this depth.

For the removal at different depths, the allowable angles of mode OBH were 2.759°, 0.969°, and 0.678°, and the ratio was 1∶0.35∶0.25. In addition, the angle decreased with

Table 3 Analytical formulas of the critical-angle fitting curve for penetration

Number	Name of envelope	Analytical formula	Formula number
1	Envelope of terminal angle for mode OBH	$\theta = -0.07h + 14.59$	(1)
2	Envelope of allowable angle for mode OBH	$\theta = -0.07h + 11.15$	(2)
3	Envelope of terminal angle for mode OBL	$\theta = -0.05h - 10.56$	(3)
4	Envelope of allowable angle for mode OBL	$\theta = -0.03h - 4.89$	(4)

Notes: In the formula above, θ is the critical angle (unit: (°)), h is depth (unit: mm). In particular, $h_0 \leqslant h \leqslant H$, where h_0 is the penetration depth caused by self-weight and H is the bucket height. In this experiment, the depth range of self-weight into the mud was 30–50 mm. The height of the skirt was 250 mm.

depth. The terminal angles of mode OBH were 2.759°, 6.035°, and 8.352°, and the ratio was 1: 2.19: 3.03. The multiple ratios of terminal and allowable angles at different depths were 1, 6.23, and 12.32. The ratio of multiple ratio was approximately 1:6:12, which changed almost linearly.

As shown in Figures 10(d), 10(e), and 10(f), the DSP curve of the mode OBL exhibited peaks at depths of 100 and 150 mm. The appearance of the second peak indicated that the soil was not completely destroyed at the first peak. Therefore, the angle at the time corresponding to the second peak point was selected as the allowable limit angle. Thus, we selected the value corresponding to the second peak point as the allowable angle. However, only one peak was observed at a depth of 50 mm for the DSP curve. Its appearance time was synchronized with the terminal angle, and thus, the values of the two critical angles were equal. For removal at different depths, the allowable angles of mode OBL were −3.288°, −6.804°, and −6.913° in sequence. Their ratio was 1:2.07:2.1. The allowable angle increased with depth. For the terminal angle at different depths, the angles of mode OBL were −3.288°, −7.805°, and −10.978° in sequence. The ratio of the three values was 1:2.37:3.34. The multiple ratios of the terminal and al-

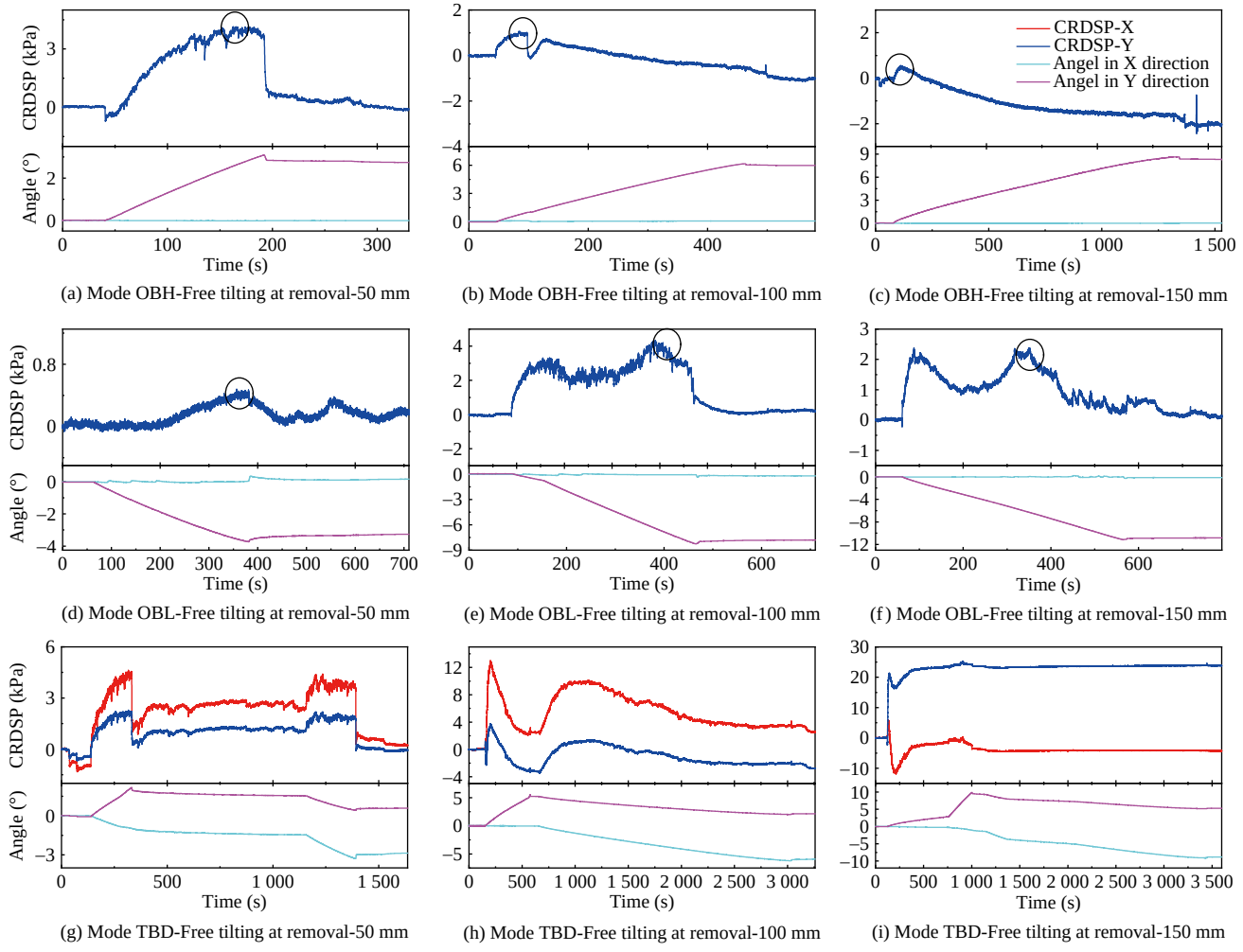

(a) Mode OBH-Free tilting at removal-50 mm (b) Mode OBH-Free tilting at removal-100 mm (c) Mode OBH-Free tilting at removal-150 mm

(d) Mode OBL-Free tilting at removal-50 mm (e) Mode OBL-Free tilting at removal-100 mm (f) Mode OBL-Free tilting at removal-150 mm

(g) Mode TBD-Free tilting at removal-50 mm (h) Mode TBD-Free tilting at removal-100 mm (i) Mode TBD-Free tilting at removal-150 mm

Figure 10 Free tilting time-history curves of CRDSP and angle during removal at different depths

lowable angles at different depths were 1, 1.15, and 1.59. The above multiple ratio was approximately 1∶1.2∶1.6, showing a nonlinear change.

Figure 10 shows that at the same depth, the critical angle of modes OBH and OBL were larger than that of the mode TBD. We drew the envelope of the critical angle, as shown in Figure 11.

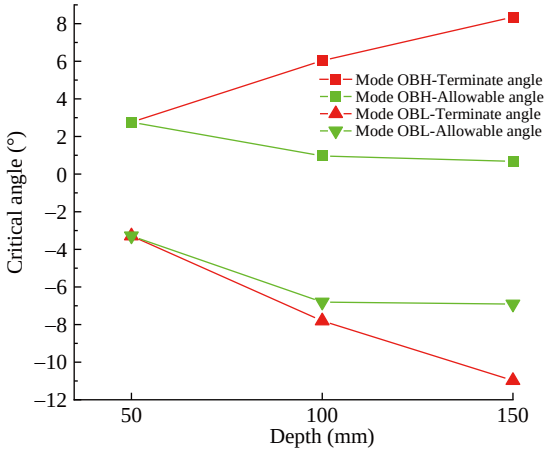

Figure 11 Critical angle-depth envelope curve of free tilting during removal

As shown in Figure 11, for removal, the terminal angle envelope was nearly linear, and the allowable angle weakened the trend from the depth of 100 mm. In the range of 50–100 mm, the slope of the allowable angle curve of the mode OBH was −0.04. However, in the range of 100–150 mm, the slope was −0.006. The former was about 6.7 times that of the latter. For the mode OBL, the slope of the allowable angle curve was −0.07 in the range of 50–100 mm. In the range of 100–150 mm, the slope was −0.002. The former slope was about 35 times that of the latter.

The allowable angle curve was nonlinear. Therefore, linear fitting was only performed on the terminal angle. Table 4 shows the analytical formula after fitting.

Table 4 Analytical formula of the critical-angle fitting curve for removal

Number	Name of envelope	Analytical formula	Formula number
1	Envelope of terminal angle for mode OBH	$\theta = 0.06h + 0.12$	(5)
2	Envelope of terminal angle for mode OBL	$\theta = -0.08h + 0.51$	(6)

4 Analysis of tilt adjustment strategy

As mentioned in Section 2.3, the test process can be divided into four stages: tilting, observation, adjustment, and watching. The monitoring of water pressure inside and outside the buckets ran through these four stages. The water pressure difference (WPD) was obtained as follows: the water pressure outside the bucket cover minus the water pressure inside the bucket cover. A positive WPD indicates suction, and a negative one indicates lift. The WPD and angle change were plotted on the same graph. According to the above four stages, the curve was divided into four regions: I, II, III, and IV. In this section, zone III was used for the analysis. The adjustment strategy was also introduced and summarized.

4.1 Analysis of water pressure during the phase of tilt adjustment

As shown in Figure 12, region III of the time-history curve was the tilt adjustment process of mode OBH. Figures 12(a), 12(c), and 12(e) exhibit the process after tilting during penetration. Figures 12(b), 12(d), and 12(f) display the process after tilting during removal. For the high-elevation bucket, at the end of the tilt adjustment, the greater the depth, the greater the value of the WPD for the No. 1 bucket.

After tilting during penetration, the high-elevation bucket was pumped for adjustment. However, seepage damage occurred around the high-elevation bucket. Therefore, water was injected into the low-elevation bucket to perform the tilt adjustment. As shown in Figures 12(a), 12(c), and 12(e), the time-history curve of the WPD of the No. 1 bucket experienced a climbing process. The greater the depth, the faster the climb. At the end of the suction tilt adjustment, the greater the depth, the greater the WPD for the No. 1 bucket. The maximum suction forces at different depths were 1.047, 2.15, and 2.817 kPa, and the ratio was 1∶2.05∶2.69. The angles corresponding to the maximum WPD (herein referred to as the Y value angle) were 11.124°, 4.629°, and 0.757°. The ratio of the Y value angle corresponding to the maximum suction position to the corresponding terminal angle was defined as the angle correction rate for suction tilt adjustment. The angle correction rates were 3.05%, 31.1%, and 82.9% at different depths. As the depth increased, the correction rate gradually increased because the shallower the burial depth, the shorter the infiltration path, and the higher the susceptibility to seepage failure. We changed the tilt adjustment method and injected water into the low-elevation bucket. The results showed that all the bucket foundations with seepage failure can be corrected back to the standard verticality range. In the water-injection stage, the fluctuation phenomenon of the WPD curve indicated that the lift was intermittently provided to the buckets. To sum up, in the case of penetration, for the angle correction of mode OBH, the shallow-buried foundation should avoid applying suction to the high-elevation bucket. Instead, the technician should inject water into the low-elevation bucket to adjust the tilt.

Figures 12(b), 12(d), and 12(f) show the condition of re-

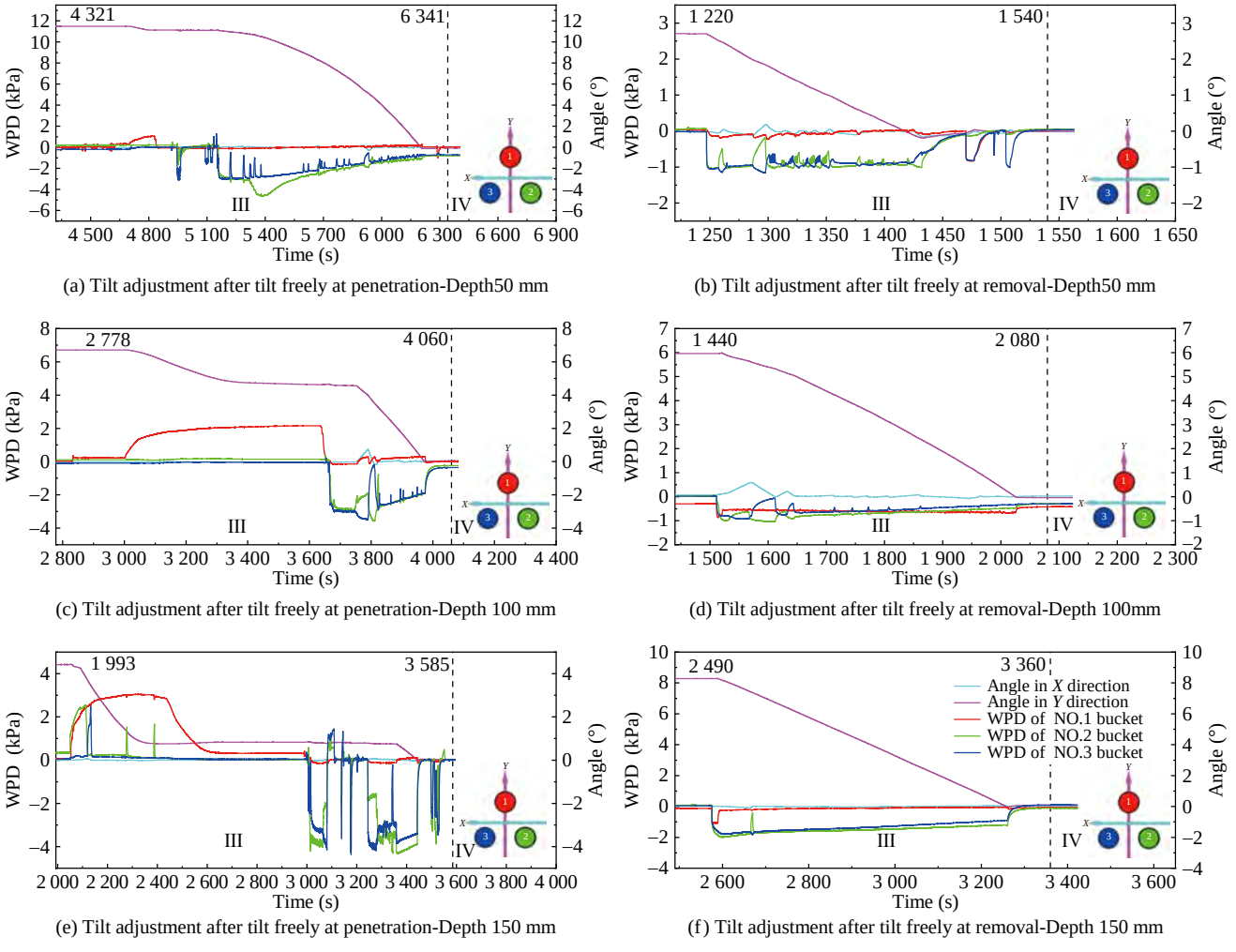

(a) Tilt adjustment after tilt freely at penetration-Depth50 mm

(b) Tilt adjustment after tilt freely at removal-Depth50 mm

(c) Tilt adjustment after tilt freely at penetration-Depth 100 mm

(d) Tilt adjustment after tilt freely at removal-Depth 100mm

(e) Tilt adjustment after tilt freely at penetration-Depth 150 mm

(f) Tilt adjustment after tilt freely at removal-Depth 150 mm

Figure 12 Tilt adjustment time curve of WPD and angle of mode OBH at different depths

moval. The tilt adjustment for mode OBH indicated that as the depth deepened, the lift value also increased. During tilt adjustment, the WPD of the bucket that was not filled with water was also negative. Thus, a bucket that is not injected with water also has lift, that is, the passive lift. Conversely, the lift generated by water injection is called the active lift. When the depth is 50 mm, the passive lift will be greater than the active lift. At a depth of 100 mm, the curves of passive and active lifts coincide. At a depth of 150 mm, the passive lift is considerably smaller than the active lift. The three buckets of the foundation were combined into a rigid body through the jacket. The water-injected bucket transmitted lift through the jacket to the uninjected bucket. Hence, passive lift occurred. According to the previous description, the greater the depth, the greater the active lift than the passive lift. The soil around the foundation has a suppressing effect on the passively moving bucket. This suppressing effect is positively correlated with the deeper burial depth of the foundation. To sum up, active lift is an effective force for tilt adjustment. The greater the foundation depth, the more force generated by water injection can be converted into an effective force for tilt adjustment.

Figure 13 shows the tilt adjustment for mode OBL. Figures 13(a), 13(c), and 13(e) reveal the penetration condition, and Figures 13(b), 13(d), and 13(f) display the removal condition. As shown in Figures 13(a), 13(c), and 13(e), suction was provided to the high-elevation bucket for tilt adjustment. At different depths, the suction power of the high-elevation bucket gradually increased with time. The maximum values of WPD at different depths were 2.05, 2.48, and 2.64 kPa, and their ratio was 1:1.2:1.29. With the increase in depth, the increasing trend of the maximum WPD decreased.

As shown in Figures 13(b), 13(d), and 13(f), for the removal condition, water was injected into the low-elevation bucket to provide lift for tilt adjustment. At a shallow depth of 50 mm, when water was injected into the low-elevation bucket, the angle in the *Y* direction was recovered, but that in the *X* direction deviated from a specification range. Thus, lift must be provided intermittently to the two high-elevation buckets to prevent the angle change in the

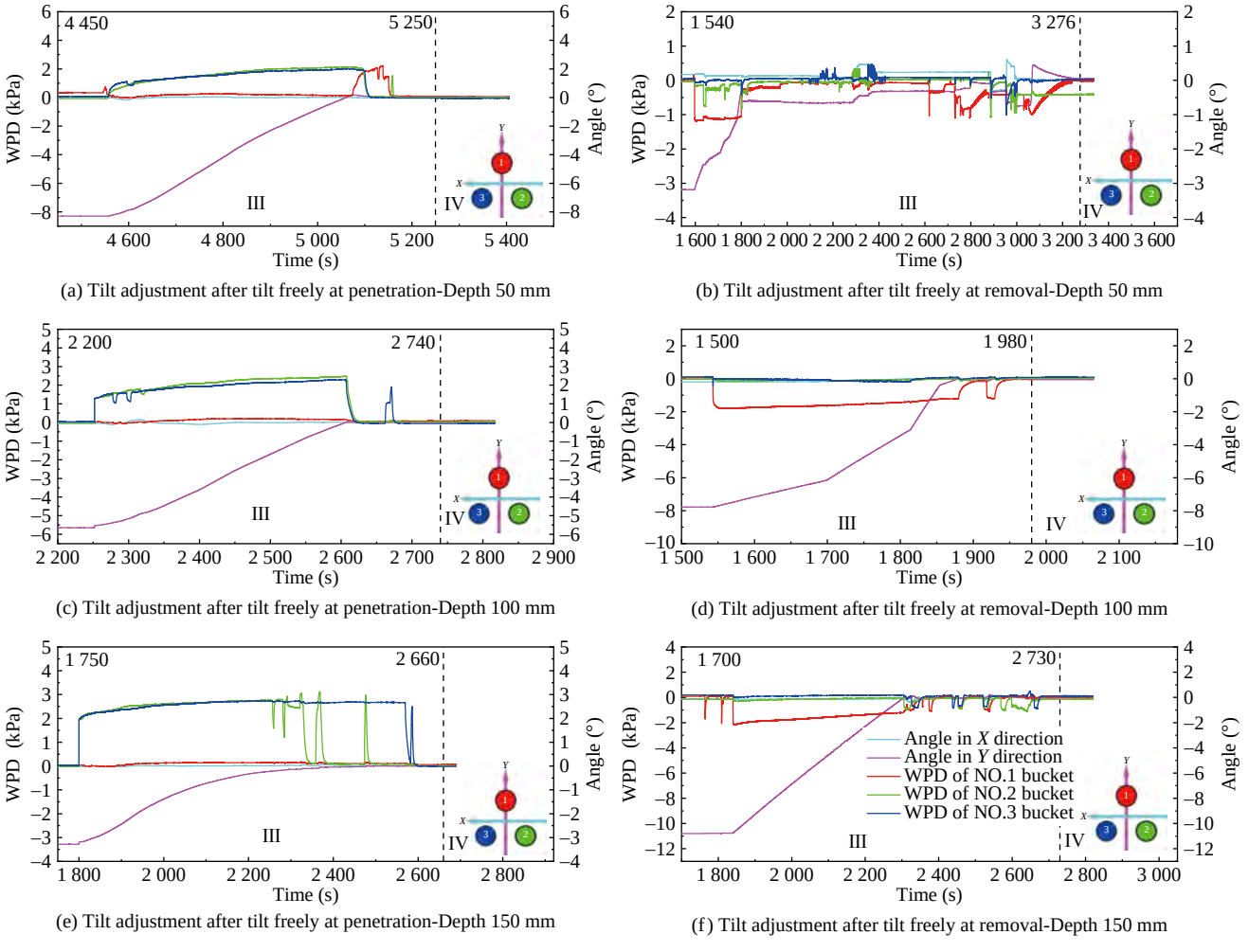

Figure 13 Tilt adjustment time curve of WPD and angle of mode OBL at different depths

X direction. However, as the depth increased, water injection for the low-elevation bucket showed minimal effect on the change in the *X*-direction angle. Thus, intermittent lift was no longer needed for the high-elevation bucket. In addition, at a depth of 100 and 150 mm, the maximum value of the WPD curve of the high-elevation bucket appeared in the initial stage. Over time, the WPD decreased with a small slope.

Figure 14 shows the tilt adjustment for mode TBD. Figures 14(a), 14(c), and 14(e) reveal the penetration condition, and Figures 14(b), 14(d), and 14(f) display the removal condition. As presented in Figures 14(a), 14(c), and 14(e), for a shallow depth of 50 mm, water was injected into the low- and mid-elevation buckets, wherein the water pressure applied to the mid-elevation bucket was lower than that applied to the low-elevation bucket. However, although the bucket had seepage damage, the foundation was still not corrected back to standard verticality. For the depth of 100 mm, suction was first applied to the high-elevation bucket (No. 1 bucket) for a certain period and then stopped. Meanwhile, water was injected into the mid- (No. 2 bucket) and low-elevation (No. 3 bucket) buckets. For the depth of 150 mm, suction was applied to the high-elevation bucket first. After a certain period, the suction supply of the No. 1 bucket was continued, and an operation was added; that is, water was injected into the low- and mid-elevation buckets. This operation aimed to prevent excessive suction for the high-elevation bucket from seepage failure.

As shown in Figures 14(b), 14(d), and 14(f), tilt adjustment was carried out for mode TBD in the removal condition. Here the bucket with the fast angle change was called the sensitive bucket. For the shallower burial depth of 50 mm, the No. 3 bucket became the sensitive bucket. Lift was provided intermittently to the sensitive bucket. The specific operation involved the repeated and rapid opening and closing of the water injection valve of the low-elevation bucket. The sensitivity of the No. 3 bucket decreased at depths of 100 and 150 mm. In addition, the greater the depth, the greater the maximum value of the WPD for the No. 3 bucket. For the WPD curve, a similar phenomenon was observed in modes OBH and OBL. The maximum WPD always appeared at the initial stage, and the WPD decreased slowly with time.

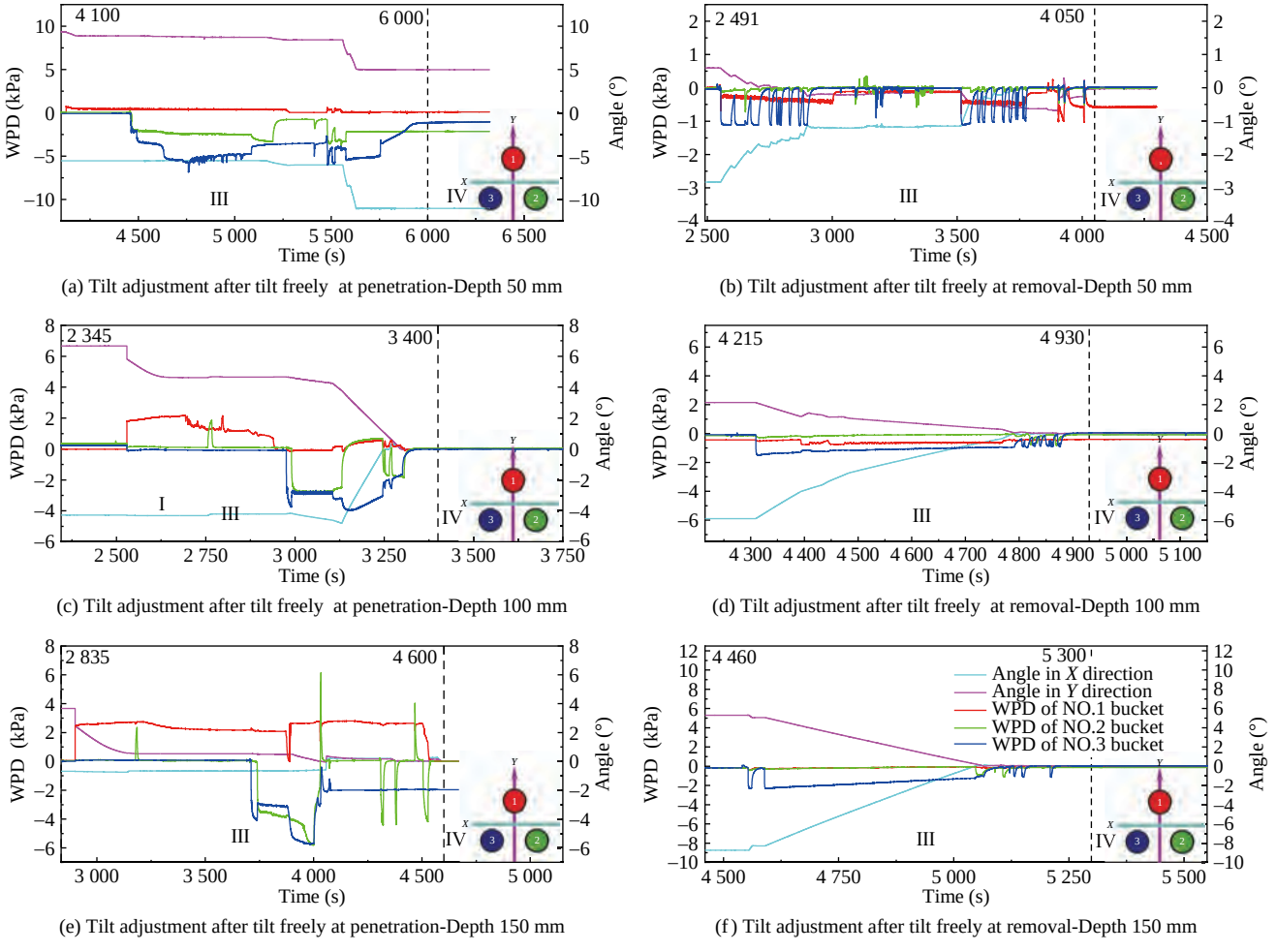

Figure 14 Tilt adjustment time curve of WPD and angle of mode TBD at different depths

4.2 Summary of tilt adjustment strategies

Figure 15 summarizes the tilt adjustment method in Section 4.1. Figures 15(a)–15(f) show the tilt adjustment method for penetration. Figures 15(g)–15(l) display the tilt adjustment method for removal. Figures 15(m)–15(o) reveal the auxiliary technique. The methods shown in Figures 15(a), 15(b), 15(g), and 15(h) exhibit the results for mode OBH. Figures 15(c), 15(d), 15(i), and 15(j) display the findings for mode OBL. Figures 15(e), 15(f), 15(k), and 15(l) illustrate the results for mode TBD. In the legend, the diameter of the circle represents bucket elevation.

As shown in Figures 15(m) and 15(n), although the No. 1 bucket exerted the same suction or lift as the other two buckets, it consistently exhibited a larger angle change. The reason for the sensitive bucket phenomenon may be the variations in soil caused by installation. Another possible cause could be a problem with the structure of the foundation itself (such as air leakage or uneven weight). The conventional solution was to reduce the applied suction or lift for the sensitive bucket. However, the force to be reduced cannot be determined in a short time. At this point, an excessively rapid response operation was required. After many attempts, the measures of the "point injection" mode can be selected. The specific operation involved controlling the valve of the sensitive bucket to repeated and rapid opening and closing. In particular, when the conventional adjustment method failed, as shown in Figure 15(o), air was injected slowly and intermittently into the low-elevation bucket. However, the injected air will cause the foundation to rise extremely fast, which may cause overturning. Therefore, engineers need to operate with caution.

In the case of the mode penetration condition, the foundation of mode OBH has reached the terminal angle. As shown in Figure 15(a), water was pumped from the high-elevation bucket first. However, around the high-elevation bucket, seepage failure easily occurred in the 12 o'clock direction (in this manuscript, the square of the *y*-axis was specified as the 12 o'clock direction). Thus, scheme 2 was executed, as shown in Figure 15(b). Instead of applying suction to the No. 1 bucket, water was injected into the low-elevation bucket. This method can successfully realize the tilt adjustment and removal of the tripod bucket jacket foundation, and it was used successfully to adjust the vertical.

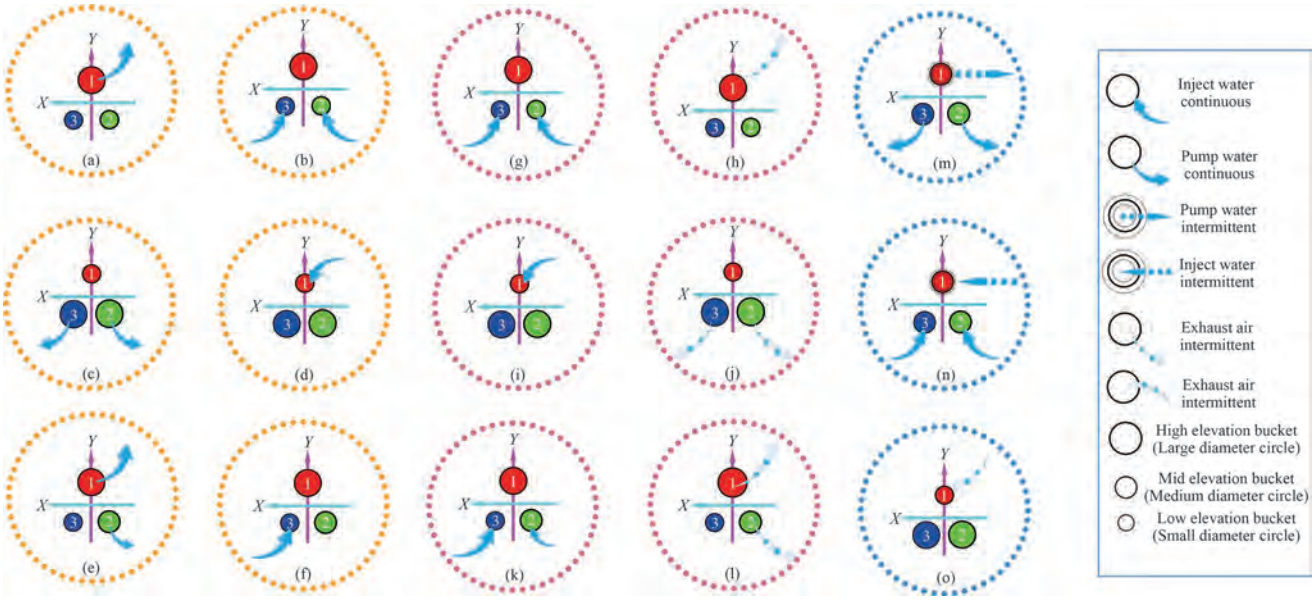

Figure 15 Summary of tilt adjustment strategy

In the case of penetration, tilt adjustment was performed on the foundation of mode OBL. Scheme 1 is shown in Figure 15(c). Suction was applied to both high-elevation buckets. The soil around No. 2 and No. 3 buckets was prone to seepage failure at 6 o'clock direction. Scheme 2 was used instead, as shown in Figure 15(d). Water was injected into the low-elevation bucket only. As a result, the foundation was successfully restored to the standard verticality range.

In the case of penetration, tilt adjustment was performed on the foundation of mode TBD. Scheme 1 is shown in Figure 15(e). Suction was applied to the high- and mid-elevation buckets, and the force applied to the former was smaller than that applied to the latter. However, this method easily induced seepage failure of the soil around the No. 1 bucket at the 1 o'clock direction. Therefore, Scheme 2 was used instead, as shown in Figure 13(f). First, lift was applied to the No. 3 bucket only. When the x-axis angle was close to returning to standard verticality, a small lift was applied to the No. 3 bucket.

Tilt adjustment for the removal situation was less complicated for the foundation of mode OBH. As shown in Figure 15(g), water was injected into two low-elevation buckets. For the foundation of mode OBL, water was injected into the low-elevation bucket only. For the foundation of mode TBD, as shown in Figure 15(k), water was injected into the low- and mid-elevation buckets. The force applied to the former should be greater than that applied to the latter. In particular, for difficult cases, the exhaust method can be used. The basis of this method is that injection water will cause more air to accumulate inside the bucket. As shown in Figures 15(h), 15(j), and 15(l), the observation hole reserved on the top cover was open, and the air was slowly released by loosening the plug.

Tilt adjustment was performed in accordance with the method shown in Figure 15. In general, the verticality can be adjusted to 2/10000, as shown in Figure 16(a). The best result is a verticality that can reach 2/100 000, as shown in Figure 16(b).

5 Conclusions

This paper explored the critical angle and tilt adjustment strategy of the tripod bucket jacket foundation by means of laboratory tests. The main conclusions are as follows:

1) In the manuscript, three possible tilt modes were discussed: OBH, OBL, and TBD. The test results demonstrated that all three modes can be corrected to verticality within a standard range. However, different strategies were required. Further, the shorter the stroke of the bucket for penetration or lifting, the more difficult the adjustment.

2) The three-bucket jacket foundation tilted during installation and removal, which caused the verticality of the foundation to change. Two critical values were considered for the tilt angle, namely, the terminal and allowable angles. When the verticality of the foundation reached the allowable angle, the soil around the bucket lost its strength. When the foundation verticality reached the terminal angle, the inclination angle did not increase.

3) In the penetration condition, the test revealed that the terminal angle was negatively correlated with the initial inclination depth. On the contrary, in the removal condition, depth was negatively correlated with the stop limit angle. In both conditions, the allowable angle was less than or equal to the terminal angle. In particular, in the penetration condition, the allowable and terminate angles changed lin-

early with the initial inclination depth. Moreover, the slopes of depth–angle curves for the two angles were approximately the same.

4) For tilt adjustment of penetration, the study summarized the sequence of measures to be used. The first strategy was to pump water from the high-elevation bucket, the second was to inject water into the low-elevation bucket, the third was to pump water from the high-elevation bucket and inject water into the low-elevation bucket, and the fourth was to inject air to the low-elevation bucket and exhaust air from the high-elevation bucket. For tilt adjustment of removal, the first strategy was to inject water into the low-elevation bucket, and the second strategy was the same as the fourth strategy of penetration. In particular, a "point injection" mode can be selected for the sensitive bucket.

Funding This research is supported by the National Natural Science Foundation of China (Grant No. 52171274).

References

Achmus M, Schroeder C (2014) Installation and bearing behaviour of bucket foundations for offshore structures. Bautechnik 91(9): 597-608. https://doi.org/ 10.1002/bate.201400043

Chen Q, Zhang P, Ding H, Le C, Xu Y (2021) Study on Seepage Characteristics of Composite Bucket Foundation Under Eccentric Load. China Ocean Engineering 35(1): 123-134. https://doi. org/ 10.1007/s13344-021-0011-6

CNS (2019) Standard for geotechnical testing method GB/T 50123-2019 (in Chinese)

Ding HY, Wang LG, Du J (2004) The model tests for adjustment of penetration of multi-bucket foundation platform. Rock and Soil Mechanics 25(3): 386-390. https://doi.org/10.3969/j.issn.1000-7598.2004.03.011

DNV (2005) Geotechnical Design and Installation of Suction Anchors in Clay Recommended Practice DNV-RP-E303

Jia N (2018) Analysis on Penetration-levelling Mechanism and Penetration Resistance of Bucket Foundation with Inner Compartments for Offshore Wind Turbines. Tianjin University.

Jia N, Zhang P, Liu Y, Ding H (2018) Bearing capacity of composite bucket foundations for offshore wind turbines in silty sand. Ocean Engineering 151, 1-11. https://doi.org/10.1016/j.oceaneng.2018.01.006

Ren Y, Vengatesan V, Shi W (2022) Dynamic Analysis of a Multi-column TLP Floating Offshore Wind Turbine with Tendon Failure Scenarios, Ocean Engineering 245, 110472. https://doi.org/10.1016/j.oceaneng.2021.110472

Wang X, Zeng X, Li J (2019) Vertical performance of suction bucket foundation for offshore wind turbines in sand. Ocean Engineering 180(4): 40-48. https://doi.org/10.1016/j.oceaneng.2019.03.049

Wu Y, Zhang Y, Li D (2020) Solution to critical suction pressure of penetrating suction caissons into clay using limit analysis. Applied Ocean Research 101,102264. https://doi.org/10.1016/j.oceaneng.2019.03.049

Zhang C (2018) Research on Penetration and Sinking-leveling of Multi Bucket Foundation for Offshore Wind Turbines. Tianjin University.

Zhang PY, Ding HY, Le CH (2013a) Model tests on tilt adjustment techniques for a mooring dolphin platform with three suction caisson foundations in clay. Ocean Engineering 73: 96-105. https://doi.org/ 10.1016/j.oceaneng.2013.08.009

Zhang PY, Ding HY, Le CH (2013b) Installation and removal records of field trials for two mooring dolphin platforms with three suction caissons. Journal of waterway, port, coastal, and ocean engineering 139(6): 502-517. https://doi.org/10.1061/(ASCE)WW.1943-5460.0000206

Zhang PY, Ding HY, Le CH (2013c) Penetration and Removal of the Mooring Dolphin Platform with Three Caisson Foundations. Journal of Offshore Mechanics and Arctic Engineering 135(4): 041302. https://doi.org/10.1115/1.4025145

Zhang PY, Zhang Z, Liu YG, Ding HY (2016) Experimental study on installation of composite bucket foundations for offshore wind turbines in silty sand. Journal of Offshore Mechanics and Arctic Engineering 138(6). https://doi.org/10.1115/1.4034456

Zhang Y, Shi W, Li DS, and Li X (2022) A novel framework for modeling floating offshore wind turbine with consideration of the dynamic effects of mooring system based on the vector form intrinsic finite element (VFIFE) method. Ocean Engineering 262: 112221. https://doi.org/10.1016/j.oceaneng.2022.112221